Electronic Supplementary information

Internal Nanoscale Architecture and Charge Carrier Dynamics of Wide Bandgap Non-Fullerene Bulk Heterojunction Active Layers in Organic Solar Cells

Xinyu Jiang[a], Hongwon Kim[a], Peter S. Deimel[b], Wei Chen[a,c], Wei Cao[a], Dan Yang[a], Shanshan Yin[a], Roy Schaffrinna[a], Francesco Allegretti[b], Johannes V. Barth[b], Martina Schwager[d], Haodong Tang[c],Kai Wang[c], Matthias Schwartzkopf[e], Stephan V. Roth[e,f], Peter Müller-Buschbaum[a,g*]

[a] Physik-Department, Lehrstuhl für Funktionelle Materialien, Technische Universität München, James-Franck-Str. 1, 85748 Garching, Germany

[b] Physik-Department, Oberflächen- und Grenzflächenphysik, Technische Universität München, James-Franck-Str. 1, 85748 Garching, Germany

[c] Department of Electrical and Electronic Engineering, Southern University of Science and Technology (SUSTech), 1088 Xueyuan Blvd. 518055 Shenzhen, China

[d] Deutsches Elektronen-Synchrotron DESY, Notkestr. 85, 22607 Hamburg, Germany

[e] Department of Applied Sciences and Mechatronics, Munich University of Applied Sciences, Lothstr. 34, 80335 München, Germany

[f] Department of Fibre and Polymer Technology, KTH Royal Institute of Technology, Teknikringen 56-58, SE-100 44 Stockholm, Sweden

[g] Heinz Maier-Leibnitz Zentrum (MLZ), Technische Universität München, Lichtenbergstr. 1, 85748 Garching, Germany

* corresponding author E-mail: muellerb@ph.tum.de

Table S1. PBDB-T-2F Bragg peaks analysis of the GIWAXS data of PBDB-T-2F:IT-M active layers

DIO (vol%)	In plane (100) q (Å^{-1})	FWHM (Å^{-1})	Int.	Out of plane (100) q (Å^{-1})	FWHM (Å^{-1})	Int.	Out of plane (010) q (Å^{-1})	FWHM (Å^{-1})	Int.
0.0	0.28 ± 0.01	0.03 ± 0.01	1091	0.30 ± 0.01	0.07 ± 0.01	1165	1.72 ± 0.01	0.32 ± 0.01	158
0.5	0.28 ± 0.01	0.04 ± 0.01	1441	0.30 ± 0.01	0.07 ± 0.01	1496	1.74 ± 0.01	0.31 ± 0.01	213
1.0	0.28 ± 0.01	0.03 ± 0.01	1094	0.30 ± 0.01	0.07 ± 0.01	1104	1.74 ± 0.01	0.33 ± 0.01	166
2.0	0.28 ± 0.01	0.03 ± 0.01	1135	0.29 ± 0.01	0.05 ± 0.01	903	1.72 ± 0.01	0.32 ± 0.01	145
				0.37 ± 0.01	0.05 ± 0.01	757			

Table S2. IT-M Bragg peaks analysis of the GIWAXS data of PBDB-T-2F:IT-M active layers

DIO (vol%)	In plane (100) q (Å^{-1})	FWHM (Å^{-1})	Int.	Out of plane (010) q (Å^{-1})	FWHM (Å^{-1})	Int.
0.0	0.31 ± 0.01	0.09 ± 0.01	273	N/A	N/A	N/A
0.5	0.31 ± 0.01	0.03 ± 0.01	614	1.86 ± 0.01	0.09 ± 0.01	25
1.0	0.31 ± 0.01	0.03 ± 0.01	507	1.87 ± 0.01	0.09 ± 0.01	21
2.0	0.30 ± 0.01	0.08 ± 0.01	336	1.86 ± 0.01	0.09 ± 0.01	16

Table S3. PBDB-T-2F crystals determined with a Gaussian model analysis of the GIWAXS data of PBDB-T-2F:IT-M active layers

DIO (vol%)	In plane (100) distance (Å)	size (Å)	Out of plane (100) distance (Å)	size (Å)	Out of plane (010) distance (Å)	size (Å)
0.0	22.4±0.1	188±1	20.9±0.1	81±1	3.7±0.1	18±1
0.5	22.4±0.1	141±1	20.9±0.1	81±1	3.6±0.1	18±1
1.0	22.4±0.1	188±1	20.9±0.1	81±1	3.6±0.1	18±1
2.0	22.4±0.1	188±1	21.7±0.1	113±1	3.7±0.1	18±1
			17.0±0.1	113±1		

Table S4. IT-M crystals determined with a Gaussian model analysis of the GIWAXS data of PBDB-T-2F:IT-M active layers

DIO (vol%)	In plane (100) distance (Å)	size (Å)	Out of plane (100) distance (Å)	size (Å)
0.0	20.3±0.1	63±1	N/A	N/A
0.5	20.3±0.1	141±1	3.4±0.1	63±1
1.0	20.3±0.1	141±1	3.4±0.1	63±1
2.0	20.9±0.1	71±1	3.4±0.1	63±1

Table S5. Gaussian fit parameters of the XPS data of the PBDB-T-2F:IT-M active layers.

DIO (vol%)	F 1s peak position (eV)	N 1s peak position (eV)	Normalized F/N Ratio*
0.0	686.2± 0.1	398.4± 0.1	1.0
0.5	685.8± 0.1	398.5± 0.1	1.0± 0.1
1.0	686.2± 0.1	398.5± 0.1	1.3± 0.2
2.0	685.9± 0.1	398.7± 0.1	2.6± 0.5

* The F/N ratios are normalized to the value for the sample with 0.0 vol% DIO addition. Individual F/N ratios were determined by using the peak area of the F 1s and N 1s core-level normalized to the specific photoionization cross section at the employed photon energy of 1253.6 eV.

Table S6. TRPL parameters of fit with a two-phase exponential decay function.

DIO (vol%)	A_1	τ_1 (ps)	A_2	τ_2 (ps)
0.0	1.20	148 ± 2	0.03	1710 ± 290
0.5	1.18	136 ± 2	0.03	1650 ± 260
1.0	1.19	150 ± 2	0.04	1590 ± 260
2.0	1.28	196 ± 2	0.03	1980 ± 450

Table S7. Electron and hole mobilities obtained by SCLC method.

DIO (vol%)	μ_h (cm^2 V^{-1} s^{-1})	μ_e (cm^2 V^{-1} s^{-1})	μ_h/μ_e
0.0	1.14 x 10^{-4}	3.59 x 10^{-7}	317.5
0.5	1.35 x 10^{-4}	1.67 x 10^{-6}	80.8

The hole and electron mobilities were determined by fitting the dark current to the model of a single carrier SCLC, which is shown by the equation:

$$J = \frac{9}{8}\varepsilon_0\varepsilon_r\mu\frac{V^2}{d^3}$$

where J is the current density, $\mu$the mobility of holes (μ_h) or electrons (μ_e), ε_0 the permittivity of the vacuum, ε_r the relative permittivity of the material and d the thickness of the blend film. V denotes the voltage $V = V_{appl} - V_{bi}$, where V_{appl} is the applied voltage, and V_{bi} the built-in potential determined by electrode work function difference. In this case, $V_{bi} = 0$ V both for hole-only and electron-only devices. The mobility was calculated from the slope of J-V plots.[1]

The hole mobility μ_h improved from 1.14 x 10^{-4} cm^2 V^{-1} s^{-1} to 1.35 x 10^{-4} cm^2 V^{-1} s^{-1} , and the electron mobility μ_e increased from 3.59 x 10^{-7} cm^2 V^{-1} s^{-1} to 1.67 x 10^{-6} cm^2 V^{-1} s^{-1} after 0.5% DIO addition. The ratio of μ_h / μ_e reduced from 317.5 to 80.8, suggesting a balanced hole and electron mobility with 0.5 vol% DIO addition.

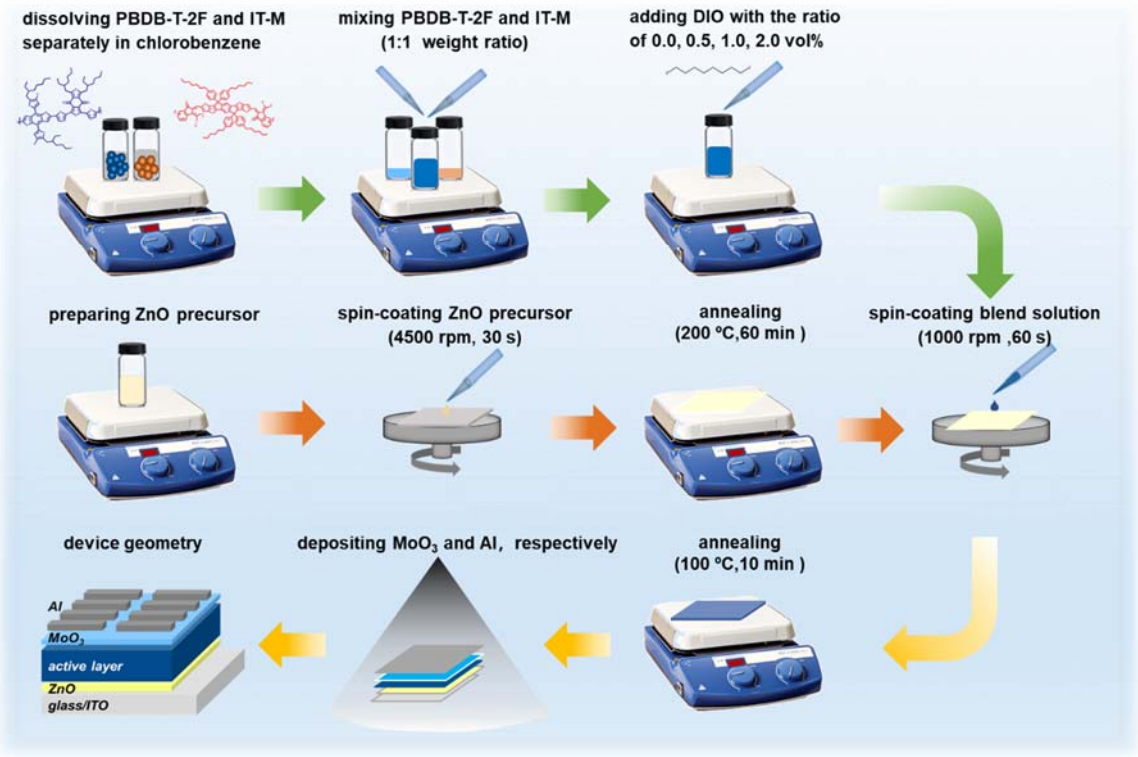

Figure S1. Details of the fabrication process of the PBDB-T-2F:IT-M based wide-bandgap non-fullerene OSC with different amounts of DIO addition.

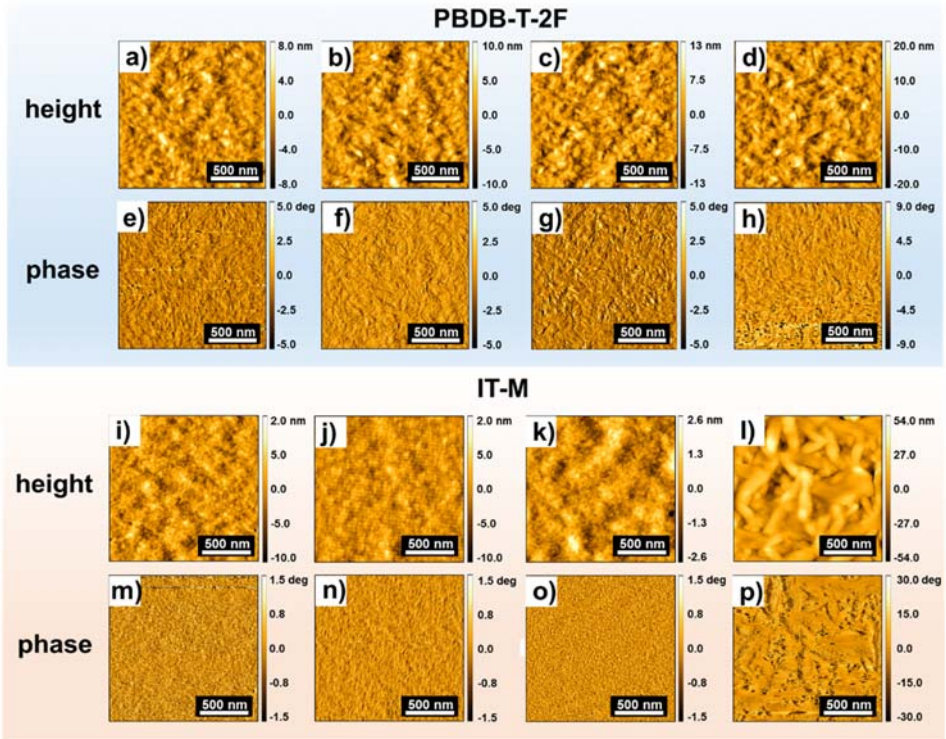

Figure S2. AFM height images of PBDBT-2F films prepared with different amounts of DIO addition (rms values) of a) 0.0 (1.4 nm), b) 0.5 (1.9 nm), c) 1.0 (2.7 nm) and d) 2.0 vol% (4.0 nm). e)-h) Corresponding phase images. AFM height images of IT-M films prepared with different amounts of DIO addition of i) 0.0 (0.3 nm), j) 0.5 (0.3 nm), k) 1.0 (0.5 nm) and l) 2.0 vol% (9.9 nm). m) -p) Corresponding phase images.

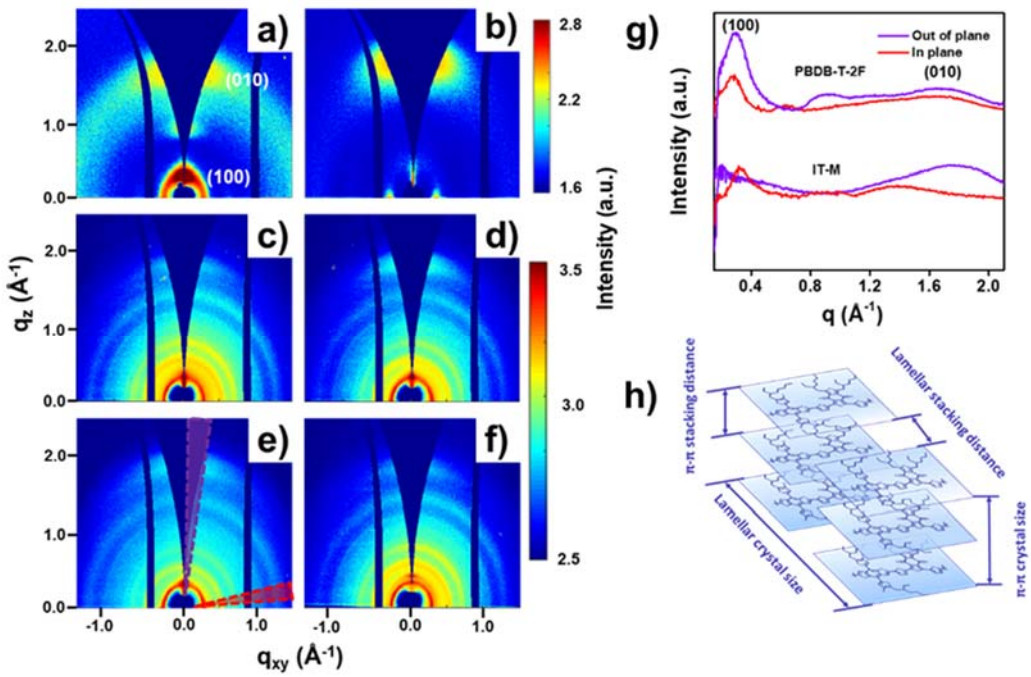

Figure S3. 2D GIWAXS data of a) PBDB-T-2F and b) IT-M films and PBDB-T-2F:IT-M active layers with c) 0.0, d) 0.5, e) 1.0 and f) 2.0 vol% DIO addition. In part e) the cake cuts are indicated in purple (out-of-plane 0º -15º) and red (in-plane 75º-90º). g) Cake cuts of 2D GIWAXS data in out-of-plane (purple line) and in-plane (red line) direction of PBDB-T-2F (top) and IT-M (bottom) films. h) Schematic diagram of lamellar and π-π stacking of PBDB-T-2F crystal. The corresponding (100) and (010) peak positions are marked.

In the out-of-plane direction, the neat PBDB-T-2F film exhibits (100), (200), and (010) Bragg reflection peaks with positions at 0.29 $Å^{-1}$, 0.61 $Å^{-1}$ and1.68 $Å^{-1}$, respectively. In the in-plane direction, the neat PBDB-T-2F film shows a (100) Bragg peak at 0.27 $Å^{-1}$ and a (010) Bragg peak at 1.60 $Å^{-1}$, suggesting both a face-on and an edge-on orientation. The IT-M thin film shows a pronounced (100) Bragg reflection peak at 0.33 $Å^{-1}$ together with a (010) Bragg peak from the π-π stacking at position of 1.8 $Å^{-1}$ in the out-of-plane direction, corresponding to a face-on orientation with respect to the substrate surface.

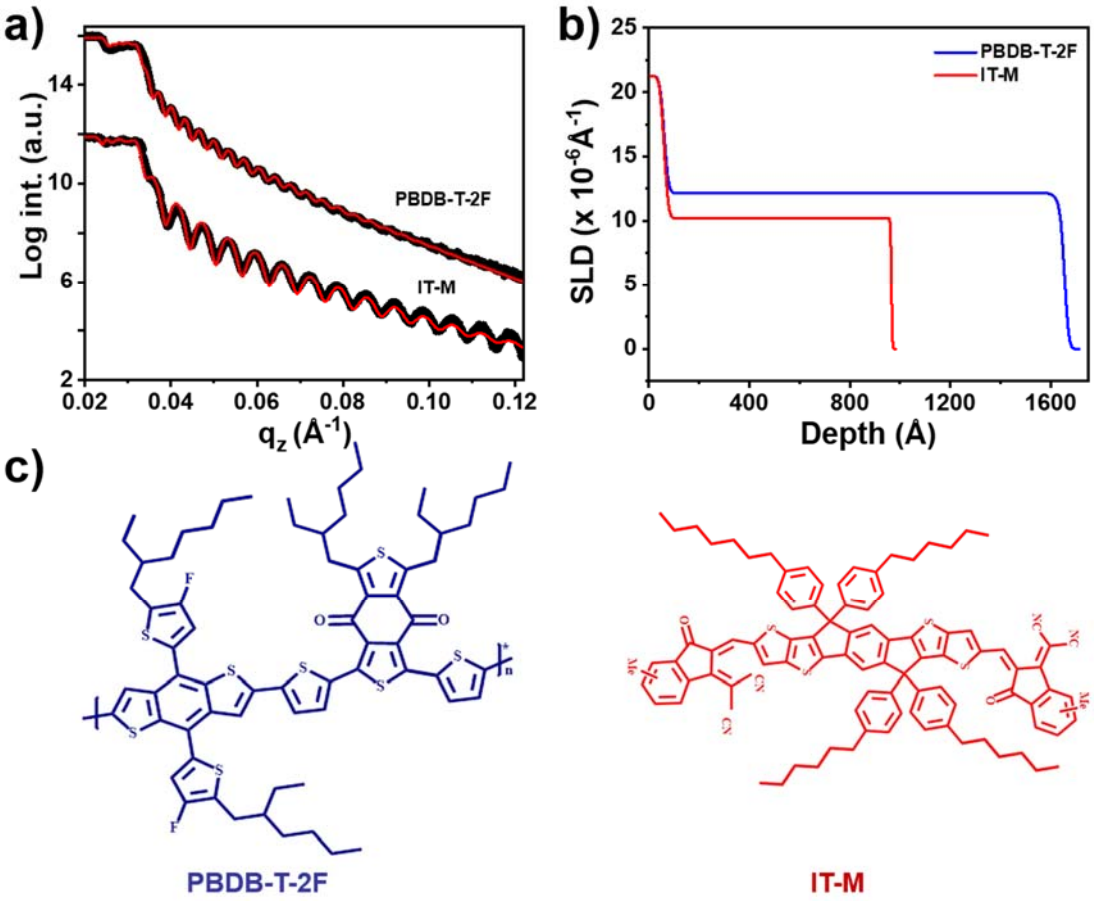

Figure S4. a) XRR data (black symbols) and corresponding fits (red lines) for neat PBDBT-2F (top) and IT-M (bottom) thin films and b) related SLD profiles. c) Chemical structure of PBDBT-2F and IT-M, respectively.

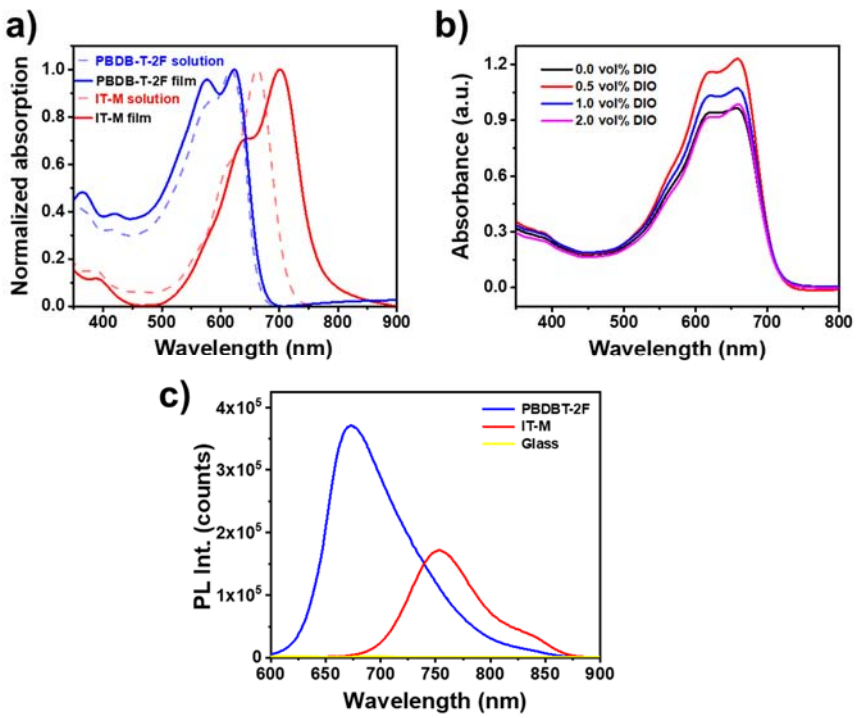

Figure S5. a) Normalized UV-vis absorption of PBDB-T-2F and IT-M in solution and in a dried thin film. b) UV-vis absorbance of diluted PBDB-T-2F: IT-M blend solutions with different DIO addition. c) PL spectroscopy data of PBDB-T-2F, IT-M films, a glass substrate, respectively.

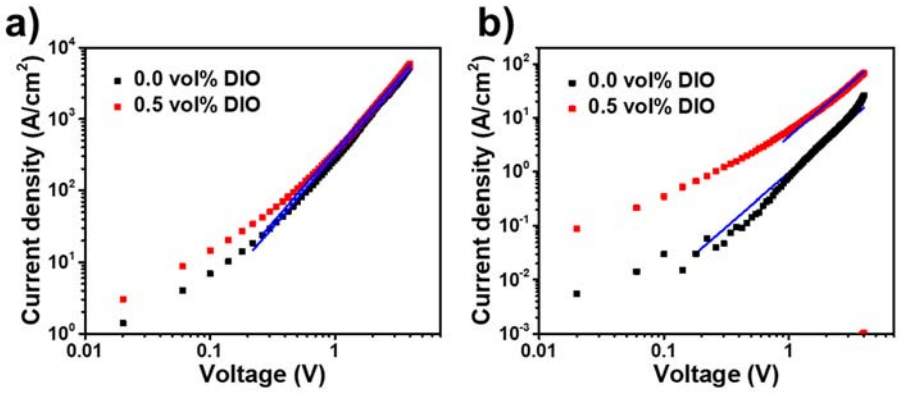

Figure S6. J-V curves as well asand the corresponding fits (blue line) for the hole-only device a) and electron-only device b), without DIO addition (black) and with 0.5 vol% DIO addition (red), respectively.

References

1. Zhang, B.; Yu, Y.; Zhou, J.; Wang, Z.; Tang, H.; Xie, S.; Xie, Z.; Hu, L.; Yip, H.-L.; Ye, L.; Ade, H.; Liu, Z.; He, Z.; Duan, C.; Huang, F.; Cao, Y. *Adv. Energy Mater.* **2020**, *10* (12), 1904247.